Characterization of Mechanical Properties of Jute/PLA Composites Containing Nano SiO2 Modified By Coupling Agents

Xueyang Song
Soochow University
Cuicui Fang
Soochow University
Yuanyuan Li
Soochow University
Ping Wang (pingwang@suda.edu.cn)
Soochow University https://orcid.org/0000-0001-6692-3850
Yan Zhang
Soochow University

Research Article

Keywords: laminating composite materials, Jute non-woven, PLA, biodegradable, nano-SiO2

Posted Date: September 20th, 2021

DOI: https://doi.org/10.21203/rs.3.rs-870428/v1

Version of Record: A version of this preprint was published at Cellulose on November 23rd, 2021. See the published version at https://doi.org/10.1007/s10570-021-04300-z.

Characterization of mechanical properties of jute/PLA composites containing nano SiO_2 modified by coupling agents

Xueyang Song, Cuicui Fang, Yuanyuan Li, Ping Wang, Yan Zhang*

National Engineering Laboratory for Modern Silk, College of Textile and Clothing Engineering, Soochow University, Suzhou, China

* Corresponding author: Yan Zhang (yanzhng86@suda.edu.cn)

Abstract: Although jute fibers-reinforced PLA composites shows strong application prospects, their low mechanical properties limit their applications to some extent. In this paper, nano-SiO_2 particles as well as modified nano SiO_2 by coupling agents which can efficiently improve the strength and toughness of composite materials are introduced into the PLA matrix. The bending, stretching and thermal properties of designed jute/PLA nonwoven composites were studied. The study shows that the nano-SiO_2 particles are beneficial to the interface performance between the PLA matrix and jute leading to improvement in the mechanical property and thermal stability. Moreover, thermomechanical properties indicate that the addition of SiO_2 can improve the jute/PLA interfacial adhesion and increase the glass transition temperature of the material. Finally, toughening mechanism of nano-SiO_2 particles in the jute/PLA composite was analyzed.

Keywords: laminating composite materials; Jute non-woven; PLA; biodegradable; nano-SiO_2

Introduction

In recent years, thermoplastic composites are increasingly applied in the high-performance engineering field due to their low density, good recyclability, and high production efficiency (Faruk et al. 2012). However, environmental compatibility of these materials is still a huge challenge. In this case, fully biodegradable green composite materials provide a feasible solution. To prepare a completely biodegradable composite material, natural fiber is a desirable reinforcing material and natural polymer can be selected as matrix material, such as jute/polylactic acid (PLA) composite materials. PLA, a polymer material, is produced from renewable agricultural raw materials. It has tremendous advantages such as high strength, high hardness, transparency and industrial production, and is one of the most promising biodegradable polymers (Qu et al. 2015). Among all biodegradable reinforced fibers, jute fiber has low cost, biodegradability and excellent mechanical property, which has made it as one of the most widely used natural plant fibers in the research of green bio-based composites (Dong et al. 2014). There are wide possible applications for jute/PLA composite, and a lot of research have been proposed to investigate its mechanical properties (Bax and Mussig 2008; Mohammed et al. 2019; Nishino et al. 2003; Pan et al. 2007). However, PLA resin matrix lacks chemical bonds and functional groups that react with jute. Therefore, the interface compatibility between jute fiber and PLA is poor, leading to a poor mechanical property of final composite. (Balla et al. 2019; Costa et al. 2012; He et al. 2019; Hossen et al. 2020; Pereira et al. 2019). At present, some physical and chemical methods have been proposed, including fiber treatment technologies such as acylation, alkali treatment, etherification and isocyanate treatment, as well as the use of coupling agents to improve the interfacial bonding properties of jute/PLA composites (Dong et al. 2020; Fang et al. 2020; Huda et al. 2007; Kumar et al. 2010; Kakroodi et al. 2012). Nano particle is also a feasible option to toughen the polymer matrix and improve the mechanical properties of fiber-reinforced composites.

In recent years, nano particles have been extensively applied to prepared composites, which has significantly improved the mechanical properties of

composites materials (Gauvin et al. 2015; Jumahat et al. 2012; Jumahat et al. 2010). Among the nanoparticles used as reinforcing materials, many researchers chose doping nano-silica (nano-SiO_2) to improve the mechanical properties of fiber-reinforced composite materials (Jumahat et al. 2015; Jumahat et al. 2012; Jumahat et al. 2010). Luo et al. (2018) used technology-resin film infusion (RFI) technology to prepare nano-SiO_2 modified carbon fiber reinforced composite materials. When the content of nano-SiO_2 is 4 wt%, the toughening and strengthening effect is the best. The tensile strength and flexural strength increased to 595.69 and 703.76 MPa, respectively, which were 86.30% and 126.98% higher than the tensile strength and flexural strength of intact sample without SiO_2. Hashim et al. (2019) studied the effect of SiO_2 nanoparticles as a reinforcing filler on the tensile response of basalt fiber reinforced polymer (BFRP) composites. It was found that the addition of SiO_2 nanoparticles showed significant improvement in tensile modulus with 6%, 14% and 19% for 5 wt%, 15 wt% and 25 wt% nano-SiO_2 content, respectively. Reddy et al. (2010) used traditional melt blending technology to prepare low nanoparticle loaded polymer composites with improved mechanical properties. The results of tensile tests indicate that the addition of SiO_2-g-DGEBA particles to the polymer matrix led to an increase of both elastic modulus and toughness (from 0.36 to 0.54 GPa, and 19.06 to 21.05 MJ/m^3, respectively). Filling nano-SiO_2 into thermoplastic matrix can combine the rigidity of nano-SiO_2 with the toughness of thermoplastic matrix, which makes ultimate composite have comprehensive mechanical performance (Hashim et al. 2019; Luo et al. 2018; Park et al. 2020).

In this study, nano-SiO_2 particles were adopted and dispersed into the PLA matrix aiming to improve the mechanical property of jute/PLA composite. Moreover, considering the dispersibility, the nano-SiO_2 was first modified with different silane coupling agents, then combined into PLA-based composite films and finally incorporated in final laminated composites. This use of sandwich-like lamination structure layer can mix PLA and jute as evenly as possible. Therefore, the effect of silane coupling agents on the mechanical property of as-prepared composites via hot-pressing technology was comprehensively analyzed.

Materials and methods

Materials

PLA (4032D; 1.24 g/cm^3) was supplied by Nature Works, USA; Jute fibers (1.45 g/cm^3) was purchased from Shandong Jiangke Linyi Co., Ltd; Nano silica (SiO_2, 99.5%, 50±5 nm) was provided by Suzhou Great Medical Technology Co., Ltd; Silane coupling agent (KH550, KH560, KH570) chemicals were provided by Jiangsu Argon Krypton Xenon Material Technology Co., Ltd. KH550 ($NH_2CH_2CH_2CH_2Si(OC_2H_5)_3$) belongs to aminosilane, KH560 ($CH_2OCHCH_2O(CH_2)_3Si(OCH_3)_3$) belongs to epoxy silane, KH570 ($CH_3CCH_2COO(CH_2)_3Si(OCH_3)_3$) belongs to formaldehyde acryloyloxy functional group silane.

Preparation of modified SiO_2

The absolute ethyl alcohol and deionized water were first mixed with a mass ratio of 9:1, and 5 g of SiO_2 was added into 100 mL of mixture. The SiO_2 solution was then sonicated in an ultrasonic cleaner for 1 h. The coupling agent, e.g. KH550, with a volume of 5% of the mixture was prepared and adjusted to the pH of 4 with oxalic acid. The above mixed solutions were magnetically stirred for 3 h at 60 ℃ for reaction. Finally, it was centrifuged (model: TG16G) and then washed with absolute ethanol solution for 3 times. The obtained precipitate was dried in an oven at 60 ℃ for 4 h to obtain modified SiO_2 powders, named as KH550-SiO_2, KH560-SiO_2 and KH570-SiO_2 respectively. The scheme of preparation process of modified SiO_2 is illustrated in Figure 1.

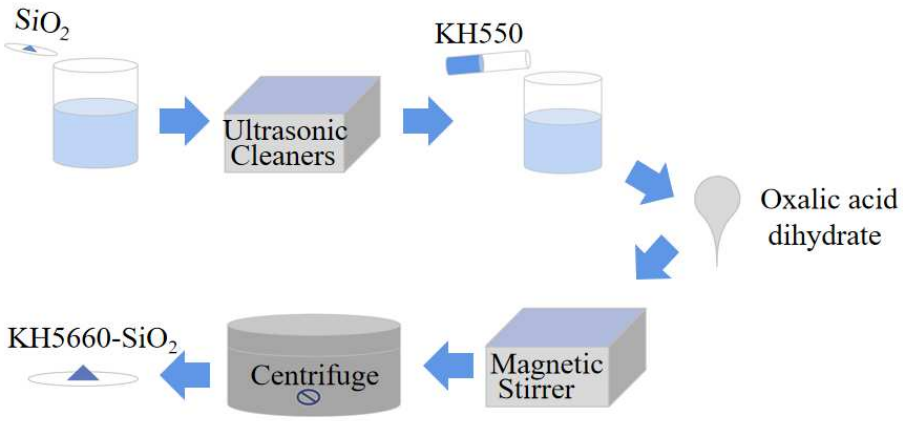

Fig. 1 The scheme of preparation process of modified SiO_2

Preparation of composite SiO_2-PLA films

3 g of PLA raw material was dissolved it in dichloromethane, stirred magnetically (model: DF-101S) for 1.5 h at room temperature; different mass fractions of modified SiO_2 (0.5 wt%, 1 wt%, 2 wt%, 4 wt% and 8 wt%) were mixed into dichloromethane and ultrasonicated (model: VGT-1730QT) for 40 min. These two solutions were mixed and magnetically stirred for 2 h, followed by ultrasonication for 1 h at 35 ℃. Then, the solution was poured into a glass plate and placed in a fume hood at room temperature to make the methylene chloride solvent completely volatilize. Finally, the composite SiO_2-PLA film was peeled from the mold and placed in a vacuum oven at a temperature of 45 ℃ for 3 h, as shown in Figure 2.

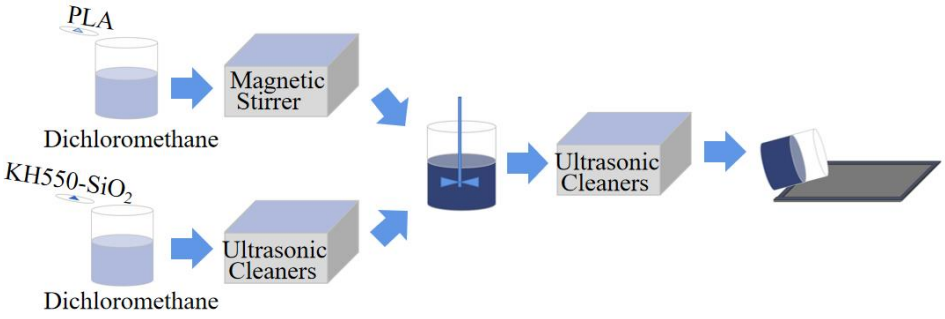

Fig. 2 The scheme of preparation process of composite SiO_2-PLA film

Preparation of jute non-woven

The preparation process of jute non-woven is shown in Figure 3. The aspect ratio

of jute fiber is about 314:1. First, the fluffy jute fibers was combed, opened and mixed through a coarse-garge carding machine (model: SSL-II) to make the fibers looser and more uniform. Then the loose jute fibers were sent to the blender for further fine opening. The fine opening and carding process make the jute fibers finally become a fluffy and uniform fiber web. The fiber web obtained by cross-netting has higher quality. In order to obtain a certain strength of non-woven fabrics, the four-layer jute net were finally reinforced with a needle punch (model: CSZC). The final thickness of the jute nonwoven is 0.51±0.04 mm, and the surface density is 200±2 g/m^2.

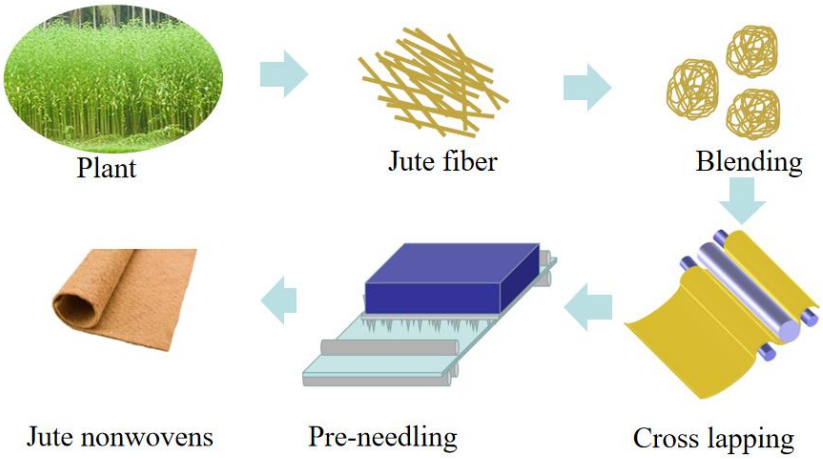

Fig. 3 The preparation process of jute non-woven fabric

Preparation of composite material

To remove all moisture, SiO_2-PLA films and jute nonwoven were first dried in a vacuum oven at 80 ℃ for 6 h before hot pressing. The laminated composite material was processed through a compression mold using a film stacking method, in which two jute pads were arranged between three PLA films in parallel, as demonstrated in Figure 4. The entire assembly was then placed in a steel mold controlled under different time and temperature. The laminated material is compacted for 0.5 h under the conditions of a temperature of 180 ℃ and a pressure of 1 MPa, and then is naturally cooled in the vulcanization machine(model: HG-3621) for 8 h. After 8 h, the sample was taken out of the laminating mold, and the width and length were 150 mm ×150 mm and the thickness was 2 mm, and the mass ratio of PLA to jute was 10:3.

The samples are numbered according to the type of coupling agent and concentration. For example, 550-0.5, in which 550 represents the silane coupling agent of KH550, the sample untreated with the coupling agent is directly represented by SiO_2, and 0.5 represents 0.5 wt% of the modified SiO_2 mass fraction in SiO_2-PLA film.

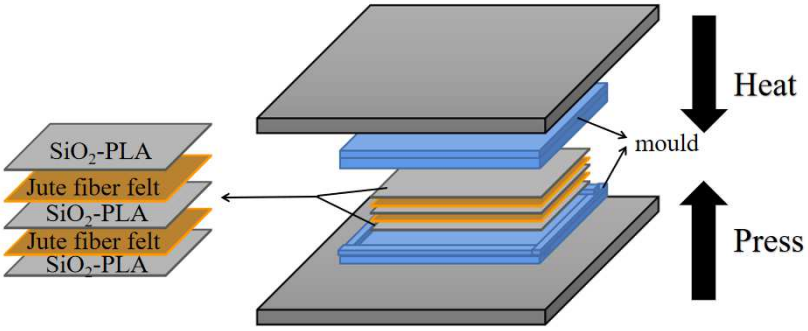

Fig. 1 The preparation process of composite material

Characterization of jute / PLA composites

In order to study that effect of different silicon dioxide on the mechanical properties of jute/PLA composite, the SiO_2 modified by silane coupling agent was characterized by infrared transmission spectroscopy (5700, Nicli Instruments, USA) and particle size analyzer (LS-909). At the same time, the mechanics of composite materials were characterized by scanning electron microscope (TM3030, Hitachi, Japan), dynamic mechanical thermal analysis (SDTQ800, V21.3, Build 96, USA) and related mechanical testing methods (Instron 336, USA).

Results and discussions

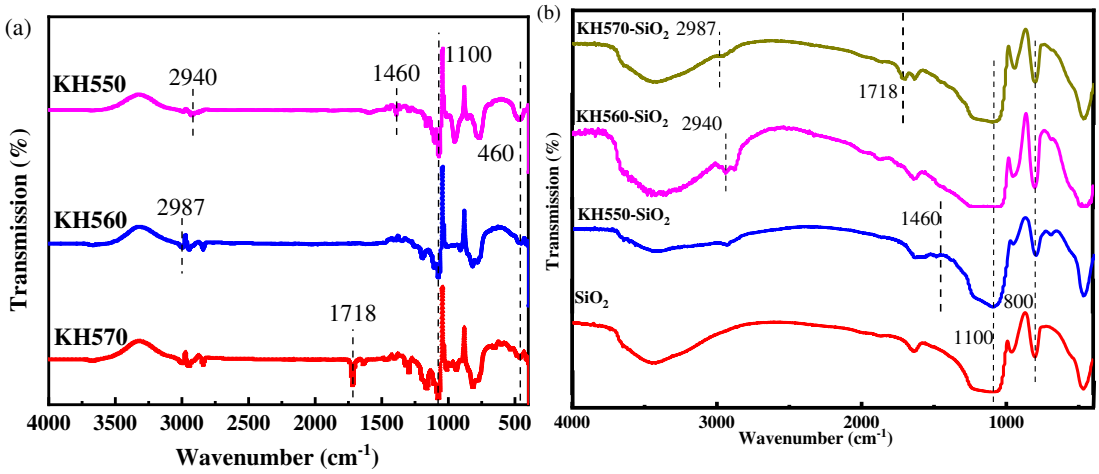

167

168 **Fig. 5** (a) FTIR spectra of KH550, KH560 and KH570; (b) FTIR spectra of SiO_2,

169 KH550-SiO_2, KH560-SiO_2 and KH570-SiO_2 nanoparticle

170

171 Fourier-transform infrared spectroscopy (FTIR) can be used to verify the graft
172 polymerization of silane coupling agents on SBR surface. Figure 5 shows the infrared
173 spectra of KH550, KH560 and KH570 as well as corresponding silane coupling agent
174 grafted SiO_2. It can be seen from Figure 5 (b) that the infrared spectrum of the SiO_2
175 before and after modification has a large absorption peak near 1100 cm^{-1}, which is the
176 antisymmetric absorption peak of Si-O-Si bond, and near 800 cm^{-1} is the symmetrical
177 contraction vibration of the Si-O-Si bond. The infrared spectrum of KH550-SiO_2 is
178 relatively flat compared to others in the range of 3500-3100 cm^{-1}, indicating that -NH_2
179 in KH550 has been successfully grafted and modified on the surface of nano-SiO_2. In
180 Figure 5 (a), KH550 shows characteristic peaks of -CH_2- at 2940 cm^{-1} and 1640 cm^{-1},
181 while KH550-SiO_2 also has a shoulder peak at 2940 cm^{-1} and 1460 cm^{-1}, which
182 further indicates that KH550 has successfully modified nano-SiO_2. Compared with
183 FTIR spectrum of SiO_2, in the spectrum modified by KH560-SiO_2, the stretching
184 vibration absorption peak of methyl appears near 2987 cm^{-1} which is related to
185 characteristic methyl peak of KH560, indicating that KH560 silane coupling agent has
186 been successfully grafted to the second Si-O surface (He et al. 2019). In the infrared
187 spectrum of KH570 and KH570-SiO_2, there is a C=O stretching vibration absorption

188 peak on the carbonyl group at 1718 cm^{-1}, which indicates that KH570 has been
189 successfully grafted onto nano-SiO_2.

190 The particle size of original and modified SiO_2 is shown in Table 1. The surface
191 morphology of original and modified SiO_2 is shown in Figure 6. Nano-SiO_2 has a
192 small particle size, a large specific surface area. Due to the large specific surface area,
193 the powder is easy to agglomerate together, so that the total surface area is reduced,
194 and the total energy is reduced. It can be clearly seen that the unmodified particles are
195 larger than modified particles, and KH560 has the best modification effect on SiO_2
196 particles. Unmodified nano-SiO_2 has a relatively high polydispersity index (PDI) and
197 the particle size, particle size, and unevenness appeared and severe aggregation. The
198 particle size and PDI of the modified nano-SiO_2 powder are reduced, indicating that
199 the nano-SiO_2 modified by the silane coupling agent can effectively prevent its
200 agglomeration and achieve the modification purpose. On the one hand, the hydroxyl
201 groups on the particle surfaces are replaced by organic functional groups, reducing the
202 number of active silanol groups, thereby reducing the tendency of nanoparticles to
203 agglomerate. On the other hand, the grafted long carbon chain increases the distance
204 between particles and the steric hindrance of the hydroxysilyl polycondensation
205 reaction on the particle surface, which increases the difficulty of effective collisions
206 and more conducive to the dispersion of nanoparticles.
207
208 **Table 1** The spectification of prepared nano SiO_2

Sample	Z-Average (nm)	Peak Size (nm)	Peak Intensity (%)	PDI
SiO_2	300	220.8	65.2	0.343
KH550-SiO_2	107.7	143.3	69.3	0.287
KH560-SiO_2	67.6	92.7	100	0.210
KH570-SiO_2	91	136.6	100	0.229

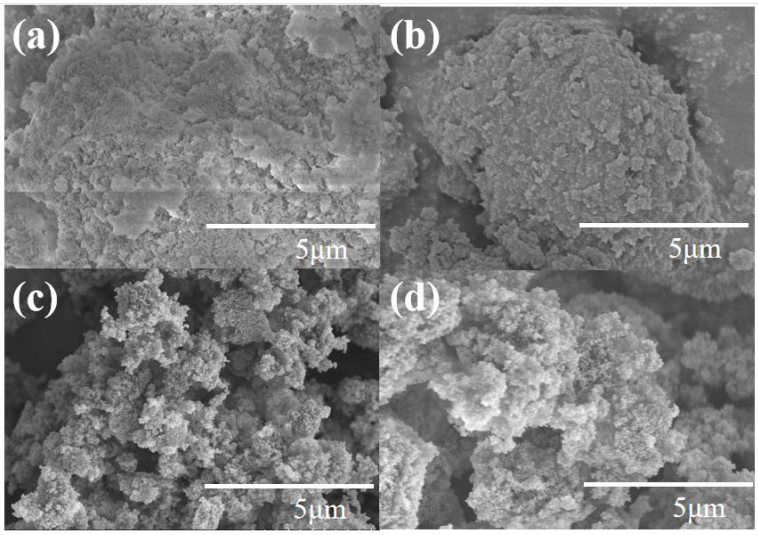

Fig. 6 The surface morphology of SiO_2. (a) SiO_2; (b) SiO_2-550; (c) SiO_2-560; (d) SiO_2-570

Bending property

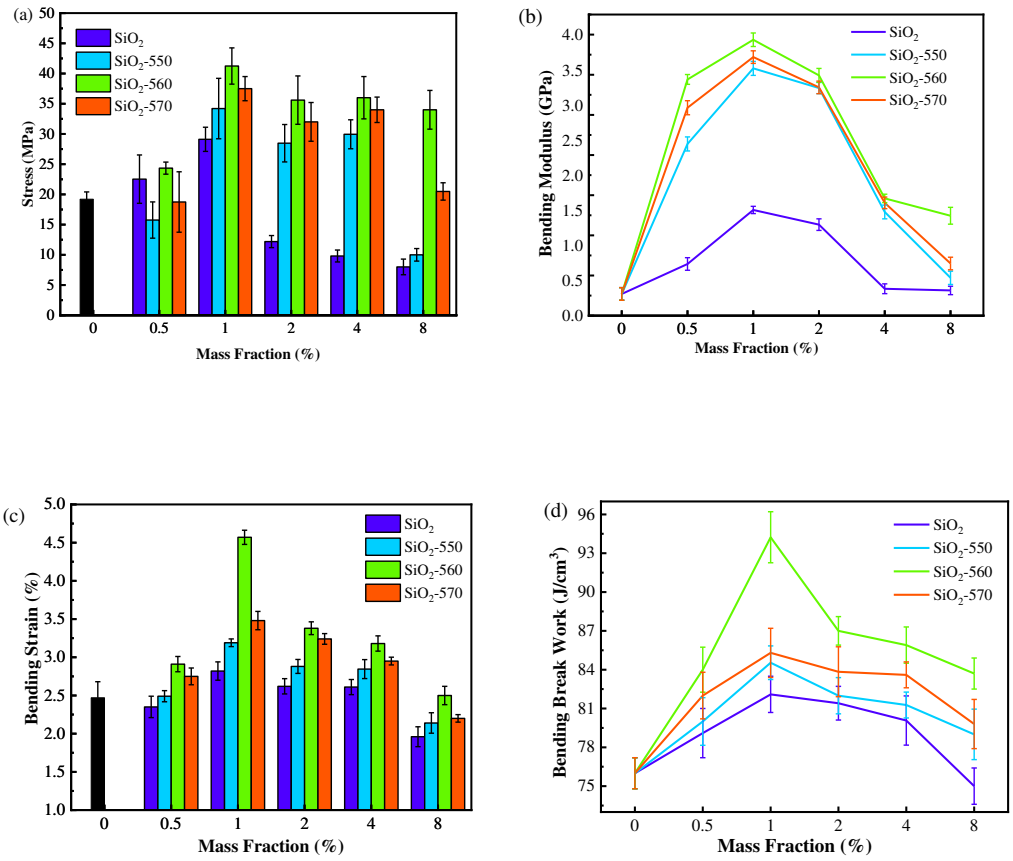

Fig. 7 The effect of nano-SiO_2 on tensile properties of jute/PLA composite bending performance. (a) Bending strength; (b) Modulus; (c) Bending strain; (d) Bending break work

The experiment was repeated at least 5 times for each sample. Figure 7 (a) and (b) shows the bending strength and modulus of pure jute/PLA fibers composites involving SiO_2 and modified SiO_2 nanoparticles with different mass fractions. It can be seen that the bending modulus of jute/PLA fibers composites is relatively low. With incorporation of SiO_2, the bending strength and modulus of the composites is more or less improved. Compared with pure jute/PLA composite material, there is no significant improvement in the bending performance of the sample SiO_2-4. However, after adding the nano-SiO_2 particles modified by the coupling agents, the bending strength and modulus of 550-4 increased to 29.95 MPa and 1.25 GPa respectively, which were 149.5% and 76.8% higher than those of the jute/PLA composite, and increased by 137.4% and 72.0% compared with the unmodified SiO_2 jute/PLA composite. The bending strength and modulus of 560-4 were increased to 36 MPa and 2.17 GPa respectively, and the bending strength and modulus of 570-4 were 34 MPa and 2.01 GPa. Compared with the jute/PLA fibers composites, the bending strength of 560-0.5, 560-1, 560-2, 560-4 and 560-8 composites increased by 2.8%, 96.6%, 74.7%, 74.2% and 68.3% respectively. It is also found from Figure 7 (a) and (b) that as the mass fraction of different types of added SiO_2 increases, the change trend of material bending strength and modulus is basically same.

The similar phenomena can be also observed in the bending strain and bending break work of jute/PLA composites. The bending break work was calculated by integrating the tensile stress–strain curves. As shown in Figure 7 (b), the increase of SiO_2 improves the bending strain and bending break work of jute/PLA composites.

In short, the bending performance of the sample increases with the increase of the SiO_2 mass fraction, peaks at about 1wt%, and then decreases. That is, under the same mass fraction, SiO_2 treated with different silane coupling agents has the same effect on the jute/PLA composite. The SiO_2 sample modified with KH560 has the best bending strength and modulus. It is mainly due to the fact that realize the interface combination through the coupling agent, forming a better entirety, and then strengthening the effect of stress transmission(Yang et al. 2009; Sanivada et al. 2020; Fang et al. 2020; Li et al. 2013). Sample 560-1 has best bending performance

248 resulting from the excellent dispersibility and uniform particle size as illustrated in
249 Table 1.
250
251 *The fracture morphology*
252 In order to illustrate the toughening mechanism, the fracture morphology of the
253 reinforced PLA-based composite after the tensile test is shown in Figure 8. The tensile
254 fracture surface of the jute/PLA composite, illustrated in Figure 8 (a), shows large
255 amounts of fiber extraction leading to a lower mechanical resistance to some extent.
256 This is consistent with comparatively large elongation ratio of the composite material
257 which also indicates a poor interfacial cohesiveness. Figure 8 (b) shows the SiO_2
258 particles modified by KH560 are evenly distributed in PLA matrix. At this time,
259 delamination occurs in the tensile section, and the bending strength is reduced. With
260 the increase of SiO_2, there are more holes appeared which are prone to cause fracture.
261 Nano-SiO_2 particles induce local plastic deformation of the PLA matrix, showing a
262 rougher fracture surface. And as the stress concentration point, SiO_2 particles produce
263 a large number of small cracks, and has a small amount of fibers extraction, as shown
264 in the Figure 8 (d). There are a large number of cracks and fiber extraction at the
265 break of sample 560-4. Therefore, sample 560-4 consumes a lot of energy when it
266 breaks. Due to the poor dispersibility of SiO_2, the modified SiO_2 re-aggregated at 8%
267 by mass fraction. As the mass fraction of SiO_2 increases, there are more contact points
268 between SiO_2 and jute, which reduces the adhesion between jute and PLA, and the
269 mechanical properties dropped rapidly, as shown in Figure 8 (f).

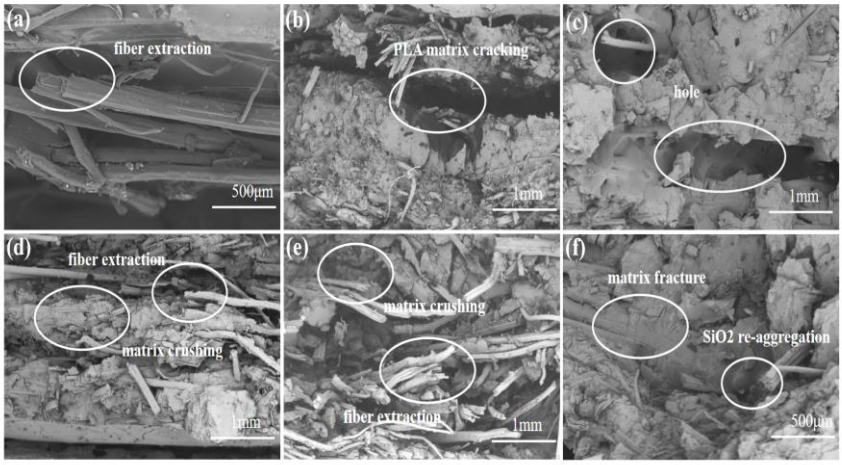

Fig. 8 The fracture surface morphologies of jute/PLA composite (×200). (a) jute/PLA composite. (b) Sample 560-0.5. (c) Sample 560-1. (d) Sample 560-2. (e)Sample 560-4. (f) Sample 560-8

Stretching property

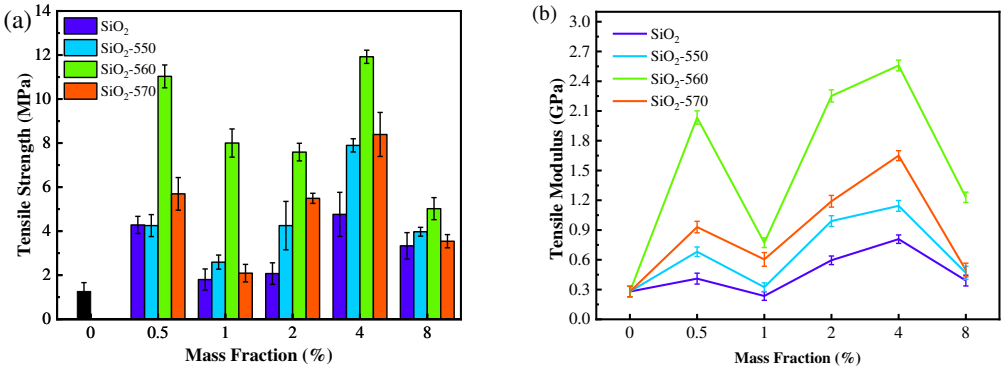

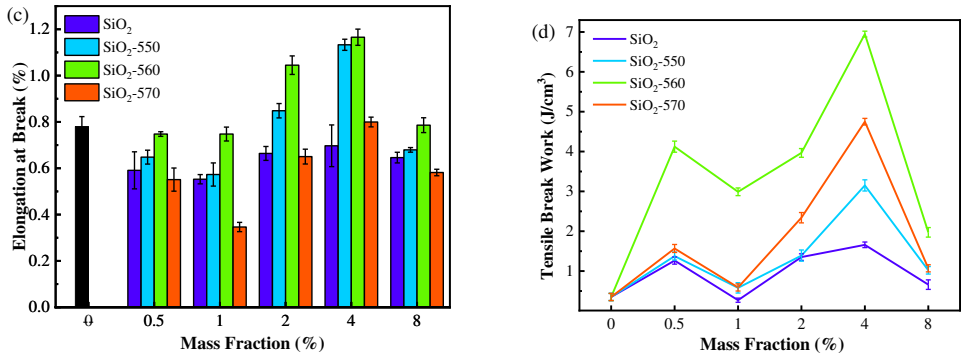

Fig. 9 The effect of nano-SiO_2 on tensile properties of jute/PLA fibers composites. (a) Tensile strength; (b)modulus; (c) Elongation at break; (d) Tensile break work

The tensile property of the jute/PLA composite and the nano-SiO_2 jute/PLA composites is shown in Figure 9. The tensile strength of 560-0.5 increased from 1.47 MPa in the jute/PLA composites to 11.03 MPa. The elastic modulus of 560-0.5 is as high as 2.01 GPa, which is 614.2% higher than the 0.28 GPa of the jute/PLA composites. The tensile strength of 560-1 is 8 MPa and the elastic modulus of 560-1 is 0.81 GPa. The tensile strength of 560-2 is 7.59 MPa and the elastic modulus is 2.32 GPa. The tensile strength of 560-4 is 11.92 MPa and the elastic modulus is 2.57 GPa. The tensile strength of 560-8 is 5.02 MPa and the elastic modulus is 1.20 GPa. The tensile break work of SiO_2-4, 550-4, 560-4, and 570-4 is increased by 138.0%, 389.7%, 609.5%, 417.0% compared with the jute/PLA fibers composites.

It is concluded from Figure 9 that the cooperation of nano-SiO_2 can effectively improve the tensile tolerance of composite materials. With the increase of nano-SiO_2 content, the change trend of the tensile properties of the composite material before and after modification is basically the same. And when the SiO_2 mass fraction is same, the sample modified by KH560 has the best tensile strength. This can be attributed to the small particle size and uniform shape of SiO_2 modified by KH560, which is consistent with the DLS data.

When preparing jute/PLA laminates, SiO_2 can be more evenly dispersed in the matrix, thereby enhancing the effective load transfer between jute and PLA, improving the tensile properties of the composite material. The silane coupling agent can serve as a bridge to improve the compatibility of the interface between SiO_2 and jute/PLA, forming a better whole, and then strengthening the stress transmission. Figure 10 shows the interaction between the silica particles and the interface of the jute/PLA composite before and after the modification. The silane coupling agent can react with the silicon hydroxyl group on the surface of SiO_2 after being hydrolyzed. The degree of aggregation of modified-SiO_2 is reduced, exposing more binding sites that can interact with PLA. At the same time, the long-chain structure of the coupling

agent will generate entanglement on the interface between jute fiber and PLA, which efficiently enhances the interface bonding performance, expedites interfacial stress transfer, and ultimately improves the mechanical property of the composite material.

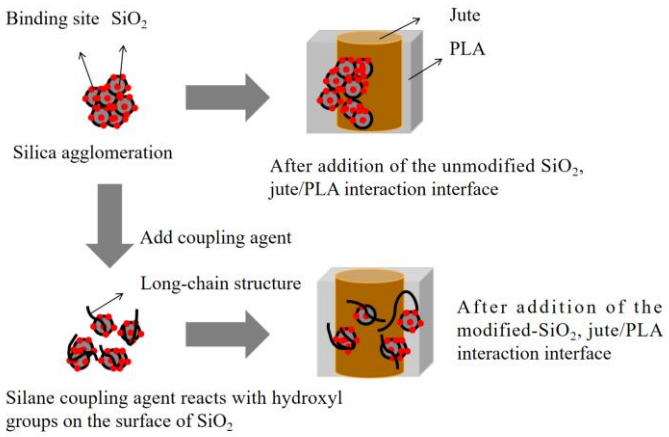

Fig. 10 The interaction between the silica particles and the interface of the jute/PLA composite before and after the modification of the silane coupling agent.

Dynamic mechanical thermal analysis (DMTA)

Figure 11 respectively show the dynamic storage modulus (E'), loss modulus (E'') and loss coefficient tanδ（E''/E'）of jute/PLA composites with different contents of SiO_2 modified from room temperature to 180 ℃. As shown in Figure 11 (a) and (b), the stored modulus values and corresponding temperatures of different samples at the beginning of chain segment movement. In the temperature range studied, the storage modulus of the jute/PLA composite modified by SiO_2 is higher than that of the untreated jute/PLA composite. In addition, different variables showed the same change pattern. With the increase of SiO_2 content, the storage modulus of the modified jute/PLA composite material increases first and then decreases. The increase in storage modulus and corresponding temperature of chain segment starting to move indicates that the interface adhesion between jute and PLA has been improved, resulting in greater stress transfer between them(Porras and Maranon. 2012). That is, the increase of the SiO_2 content can improve the interfacial adhesion, but because of the poor dispersibility of SiO_2, when the content is greater than 4%, the effect of the

coupling agent on SiO_2 modification is not obvious, and the jute/PLA interface adhesion begins to decrease.

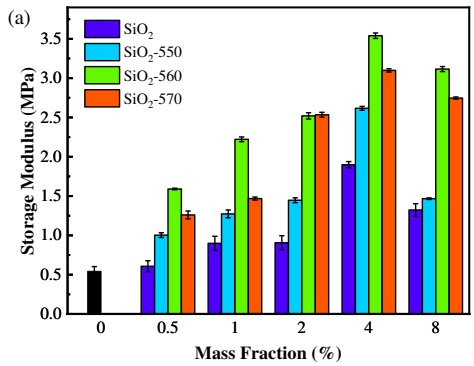

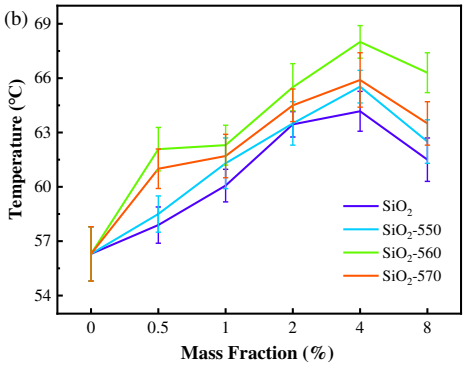

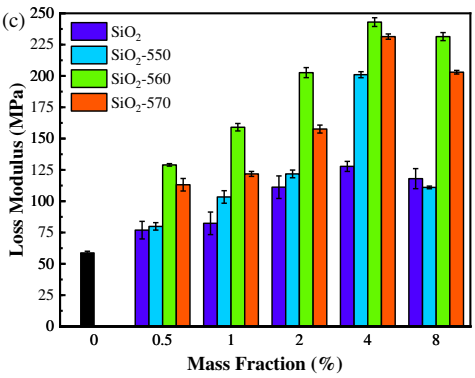

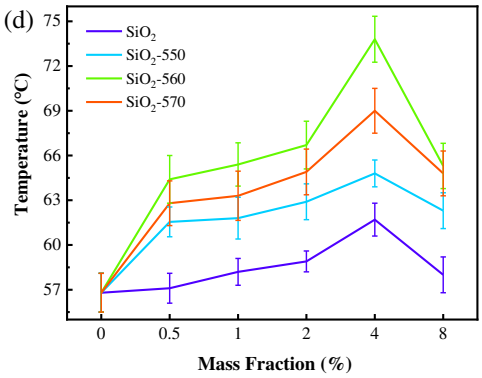

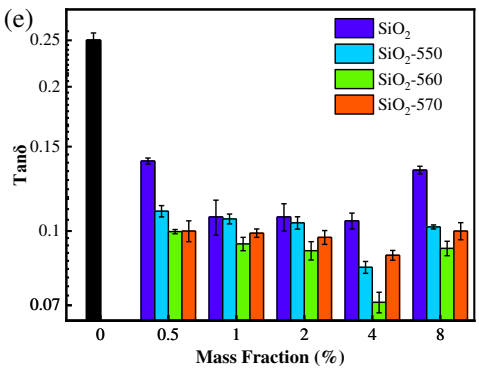

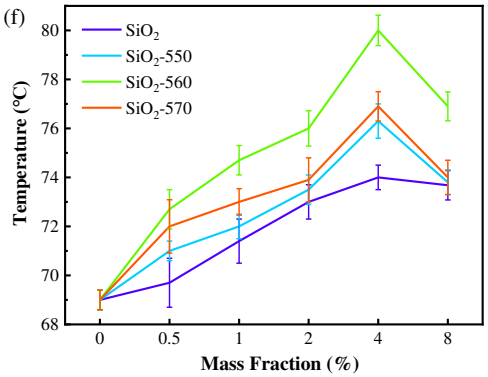

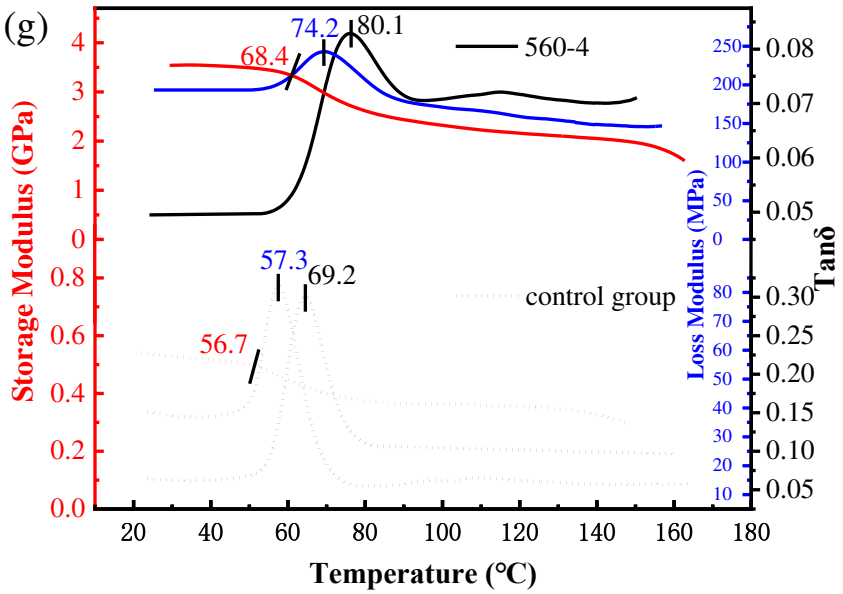

Fig. 11 The DMTA of jute/PLA composite. (a) Storage modulus; (b) The temperature corresponding to storage modulus; (c) The maximum loss modulus; (d) The temperature corresponding to the maximum loss modulus; (e) The maximum tanδ; (f) The temperature corresponding to the maximum tanδ; (g) The comparison of DMTA between jute/PLA composite and sample 560-4

The next study parameter is the loss modulus, which represents the energy dissipated by the jute/PLA composite under stress (Laly et al. 2003; Doan et al. 2007). It is observed in Figure 11 (c) and (d) that the loss modulus value of the SiO_2-modified jute/PLA composite is much higher than that of the untreated jute/PLA composite. It is known that the maximum value of loss modulus corresponds to the glass transition temperature (Tg) of the composite material. The Tg of the untreated jute/PLA composite is around 57.3 ℃. In contrast, the Tg of the SiO_2-modified jute/PLA composite material moved to the high temperature zone, reaching a maximum of about 74.2 ℃.

Finally, loss factor, tanδ, which refers to the ratio of the loss modulus of the composite material to the storage modulus of the composite material, and represents

the damping energy of the material. The decrease of the tanδ value indicates SiO_2 improves the bonding strength between PLA and jute, and reduces the fluidity of PLA macromolecules in the composite material. Due to the improvement of the hydrophobicity of the SiO_2-modified Jute/PLA, the interfacial adhesion is enhanced, and the fluidity of the polymer chains at the jute/PLA composite interface is reduced. Among the unmodified SiO_2 and SiO_2 jute/PLA composites modified by KH550, KH560 and KH570, the unmodified jute/PLA composites have the highest tanδ value, and the KH560 modified SiO_2 jute/PLA composites has the highest tanδ value, indicating the dispersibility of SiO_2 modified by KH560 is best. Among all SiO_2 composite material modified by KH560, jute/PLA with a SiO_2 content of 4% has the best interface bonding. As shown in Figure 11 (e) and (f).

Comprehensive analysis of sample 560-4 has the best thermomechanical properties. Compared with the jute/PLA composite, the storage modulus, glass transition temperature and loss modulus have increased; tanδ has decreased. As shown in Figure 11 (g), the comparison of DMTA between jute/PLA composite and sample 560-4. The glass transition temperature of sample 560-4 is 29.5% higher than that of the jute/PLA composite, indicating that the experimental optimization has improved the bonding strength of the interface between PLA and jute. The storage modulus values of different samples decrease with increasing temperature. The tanδ value of the jute/PLA composite material increased with the increase of temperature when the mass fraction of SiO_2 treated by KH560 was 4%, until it reached the maximum at 69.2℃, and then the opposite trend was observed in the rubber area.

Conclusions

In order to enhance the mechanical properties of the jute/PLA composite, nano-SiO_2 particles modified by different coupling agents were introduced into the PLA matrix. The effect of the type of coupling agent and the mass fraction of SiO_2 on the bending, stretching and thermomechanical properties of the composite was studied. The study shows that the addition of SiO_2 improves the interface performance between PLA and jute and improves the mechanical properties of the composite

material. Meanwhile, the smaller the particle size of SiO_2 and the more uniform the particles, the better the mechanical properties of the composite material. The analysis of thermomechanical properties shows that the addition of SiO_2 can improve the thermomechanical properties and glass transition temperature of composite materials. In addition, as shown in the tensile and bending tests, the strength, stiffness and toughness of SiO_2 composite material with mass fraction of 4% modified by the KH560 coupling agent are significantly improved, and its elongation at break is slightly affected. Compared with intact jute/PLA composite, the flexural strength and flexural modulus of sample 560-4 increase by 150.3% and 77.4%, respectively, while the tensile strength and tensile modulus increase by 816.9% and 700.1%, respectively. Its excellent mechanical properties are the result of the better interface compatibility of jute/PLA caused by the SiO_2-CN bond. In addition, the fracture morphology of the composite material shows that the plastic deformation of the matrix caused by SiO_2 are the main toughening mechanisms.

In summary, adding SiO_2 modified by coupling agent to jute/PLA composites can improve the mechanical properties of composites, which can be used in packaging, automotive and other industries. Make products more green and environmentally friendly.

Acknowledgements

The work is gratefully supported by National Natural Science Foundation of China (Grant No.11602156), Science and Technology Guiding Project of China National Textile and Apparel Council (Grant No. 2020064).

Declaration of competing interest

The authors declare that they have no known competing financial interests or personal relationships that could have appeared to influence the work reported in this paper.

References

Bax B, Mussig J (2008) Impact and tensile properties of PLA/cordenka and PLA/flax

composites. Composites Science and Technology 68(7-8):1601-1607. https://doi.org/10.1016/j.compscitech.2008.01.004

Balla VK, Kate KH, Satyavolu J, et al (2019) Additive manufacturing of natural fiber reinforced polymer composites: Processing and prospects. Composites Part-B Engineering 174:106956. https://doi.org/10.1016/j.compositesb.2019.106956

Costa S, Ferreira D, Ferreira A, et al (2012) Multifunctional flax fibres based on the combined effect of silver and zinc oxide (Ag/ZnO) nanostructures. Nanomaterials 8(12):1069. https://doi.org/10.3390/nano8121069

Cheon J, Kim M (2021) Impact resistance and interlaminar shear strength enhancement of carbon fiber reinforced thermoplastic composites by introducing MWCNT-anchored carbon fiber. Composites Part B: Engineering 217:108872. https://doi.org/10.1016/j.compositesb.2021.108872

Doan TTL, Brodowsky H, Mader E (2007) Jute fibre/polypropylene composites II. Thermal, hydrothermal and dynamic mechanical behaviour. Composites Science and Technology 67(13):2707-2714. https://doi.org/10.1016/j.compscitech.2007.02.011

Dong Y, Ghataura A, Takagi H, et al (2014) PLA biocomposites reinforced with coir fibres: evaluation of mechanical performance and multifunctional properties. Composites Part A: Applied Science and Manufacturing 63(18):76-84. https://doi.org/10.1016/j.compositesa.2014.04.003

Dong Y, Ghataura A, Takagi H, et al (2014) PLA biocomposites reinforced with coir fibres: evaluation of mechanical performance and multifunctional properties. Composites Part A: Applied Science and Manufacturing 63(18): 76-84. https://doi.org/10.1016/j.compositesa.2014.04.003

Dong AX, Wu HM, Liu RR, et al (2020) Horseradish peroxidase-mediated functional hydrophobization of jute fabrics to enhance mechanical properties of jute/thermoplastic composites PLA biocomposites reinforced with coir. Polymer Engineering and Science 2020: 25612. https://doi.org/10.1002/pen.25612

Faruk O, Bledzki AK, Fink HP, et al (2012) Biocomposites reinforced with natural fibers: 2000-2010. Progress in Polymer Science 37(11):1552-1596.

https://doi.org/10.1016/j.progpolymsci.2012.04.003

Fang CC, Zhang Y, Qi SY, et al (2020) Characterization and analyses of degradable composites made with needle-punched jute nonwoven and polylactic acid (PLA) membrane. Cellulose 27(10):5971-5980. https://doi.org/10.1007/s10570-020-03204-8

Fang CC, Zhang Y, Qi SY, et al (2020) Influence of structural design on mechanical and thermal properties of jute reinforced polylactic acid (PLA) laminated composites. Cellulose 27(16):9397-9407. https://doi.org/10.1007/s10570-020-03436-8

Gauvin F, Cousin P, Robert M (2015) Improvement of the interphase between basalt fibers and vinylester by nano-reinforced post-sizing. Fibers and Polymer 16(2):434-442. https://doi.org/10.1007/s12221-015-0434-x

Huda MS, Drzal LT, Mohanty AK, et al (2007) Effect of fibers surface-treatments on the properties of laminated biocomposites from poly (lactic acid) (PLA) and kenaf fibers. Composites Science and Technology 68(2):424-432. https://doi.org/10.1016/j.compscitech.2007.06.022

He H, Tay TE, Wang Z, et al (2019) The strengthening of woven jute fibers/polylactide biocomposite without loss of ductility using rigid core–soft shell nanoparticles. Journal of Materials Science 54(6):4984-4996. https://doi.org/10.1007/s10853-018-03206-9

Hashim UR, Jumahat A, Mahmud J (2019) Improved tensile properties of basalt fibre reinforced polymer composites using silica nanoparticles. Materialwissenschaft und Werkstofftechnik 50(9):1149-1155. https://doi.org/10.1002/mawe.201800071

Hossen M, Feng J, Yuxiang Y, et al (2020) Preparation and evaluation mechanical, chemical and thermal properties of hybrid jute and coir fibers reinforced bio-composites using poly-lactic acid and poly-caprolactone blends. Materials Research Express 7(2):025103. https://doi.org/10.1088/2053- 1591/ab952b

Kumar R, Yakabu MK, Anandjiwala RD (2010) Effect of montmorillonite clay on flax fabric reinforced poly lactic acid composites with amphiphilic additives.

473 Composites Part A-Applied Science and Manufacturing 41(11):1620-1627.
474 https://doi.org/10.1016/j.compositesa.2010.07.012
475 Kakroodi AR, Bainier J, Rodrigue D (2012) Mechanical and morphological properties
476 of flax fibers reinforced high density polyethylene/recycled rubber composites.
477 International Polymer Processing 27(2):196-204.
478 https://doi.org/10.3139/217.2473
479 Laly AP, Zachariach O, Sabu T (2003) Dynamic mechanical analysis of banana fibers
480 reinforced polyester composites. Composites Science and Technology
481 63(2):283-293. https://doi.org/10.1016/S0266-3538(02)00254-3
482 Li X, Lei B, Lin Z, et al (2013) The utilization of bamboo charcoal enhances wood
483 plastic composites with excellent mechanical and thermal properties. Materials
484 and Design 53(1):419-424. https://doi.org/10.1016/j.matdes.2013.07.028
485 Luo H, Ding J, Huang Z, et al (2018) Investigation of properties of nano-silica
486 modified epoxy resin films and composites using RFI technology. Composites
487 Part B 155:288-298. https://doi.org/10.1016/j.compositesb.2018.08.055
488 Jumahat A, Soutis C, Jones FR, et al (2010) Effect of silica nanoparticles on
489 compressive properties of an epoxy polymer. Journal of Materials Science
490 45(21):5973-5983. https://doi.org/10.1007/s10853-010-4683-1
491 Jumahat A, Soutis C, Mahmud J, et al (2012) Compressive properties of
492 nanoclay/epoxy nanocomposites. Procedia Engineering 41:1607-1613.
493 https://doi.org/10.1016/j.proeng.2012.07.357
494 Jumahat A, Soutis C, Abdullah SA , et al (2012) Tensile properties of
495 nanosilica/eepoxy nanocomposites. Procedia Engineering 41:1634-1640.
496 https://doi.org/10.1016/j.proeng.2012.07.361
497 Jumahat A, Kasolang S, Ba Hari MT (2015) Wear properties of nanosilica filled
498 epoxy polymers and FRP composites. Jurnal Tribologi 6:24-36.
499 Mohammed L, Ansari MNM, Pua G, et al (2019) A review on natural fibers reinforced
500 polymer composite and its applications. International Journal of Polymer Science
501 2015:243947. https://doi.org/10.1155/2015/243947
502 Nishino T, Hirao K, Kotera M, et al (2003) Kenaf reinforced biodegradable composite.

503 Composites Science and Technology 63(9):1281-1286.
504 https://doi.org/10.1016/s0266-3538(03)00099-x
505 Pan PJ, Zhu B, Kai W, et al (2007) Crystallization behavior and mechanical properties
506 of bio-based green composites based on poly(L-lactide) and kenaf fibers. Journal
507 of Applied Polymer Science 105(3):1511-1520.
508 https://doi.org/10.1002/app.26407
509 Porras A, Maranon A (2012) Development and characterization of a laminate
510 composite material from polylactic acid (PLA) and woven bamboo fabric.
511 Composites Part B Engineering 43(7):2782-2788.
512 https://doi.org/10.1016/j.compositesb.2012.04.039
513 Pereira JF, Ferreira DP, Pinho E, et al (2019) Chemical and biological warfare
514 protection and self-decontaminating flax fabrics based on CaO nanoparticles.
515 Key Engineering Materials 812(1):75-83.
516 https://doi.org/10.4028/www.scientific.net/kem.812.75
517 Park JE, Seok BY (2020) Mechanical properties of inorganic particle reinforced
518 epoxy composites for gas insulated switchgear. Journal of Mechanical Science
519 and Technology 34(7):2795-2799. https://doi.org/10.1007/s12206-020-0612-7
520 Qu P, Gao Y, Wu GF, et al (2015) Nanocmposites of poly (lactic acid) reinforced with
521 cellulose nanofibrils. Bioresources 5(3):1811-1823.
522 Reddy CS, Das CK, Narkis M (2010) Propylene-ethylene copolymer nanocomposites:
523 epoxy resin grafted nanosilica as a reinforcing filler. Polym Compos
524 26(6):806-12. https://doi.org/10.1002/pc.20145
525 Sanivada UK, Gonzalo M, Brito FP, et al (2020) PLA composites reinforced with flax
526 and jute fibers-A review of recent trends, processing parameters and mechanical
527 properties. Polymers 12(10):2373. https://doi.org/10.3390/polym12102373
528 Wang D, Xuan L, Han G, et al (2020) Preparation and characterization of foamed
529 wheat straw fiber/polypropylene composites based on modified nano-TiO2
530 particles. Composites Part A Applied Science and Manufacturing 128:105674.
531 https://doi.org/10.1016/j.compositesa.2019.105674
532 Yang HF, Li FH, Shan CS, et al (2009) Covalent functionalization of chemically

533 converted graphene sheets via silane and its reinforcement. Journal of Materials
534 Chemistry 19(26):4632-4638. https://doi.org/10.1039/b901421g

Figures

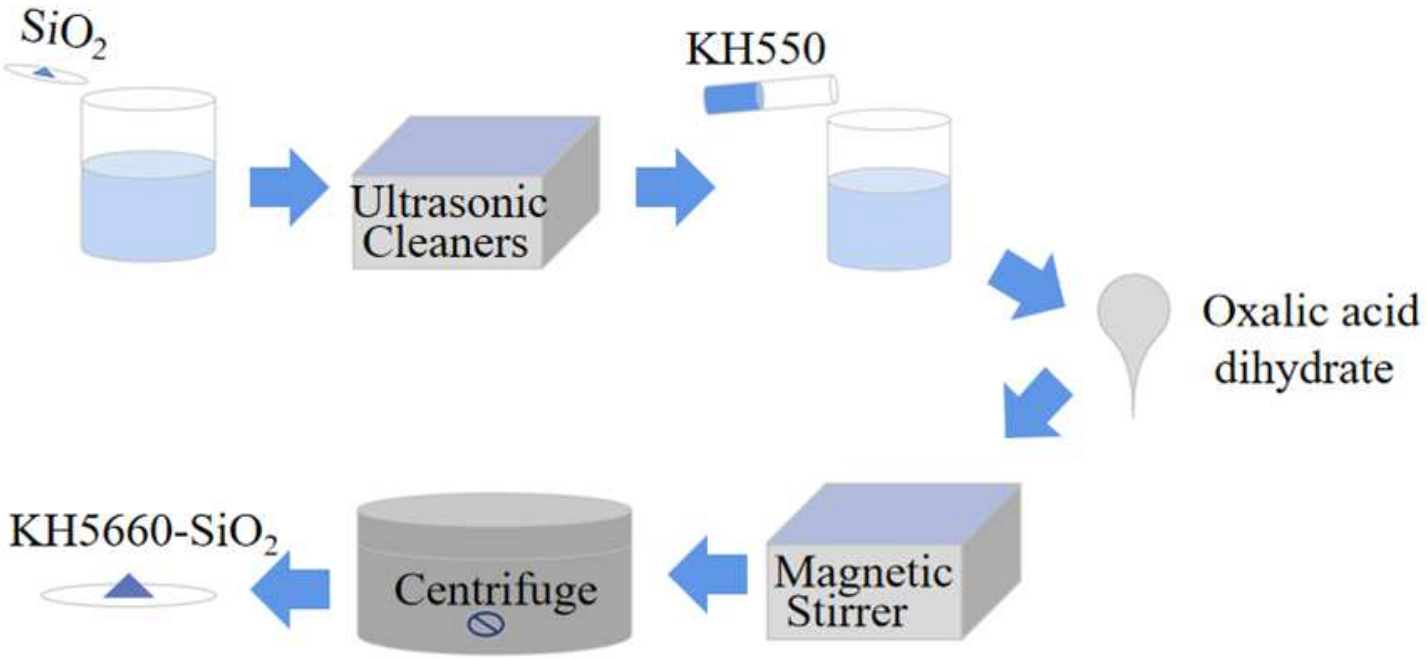

Figure 1

The scheme of preparation process of modified SiO2

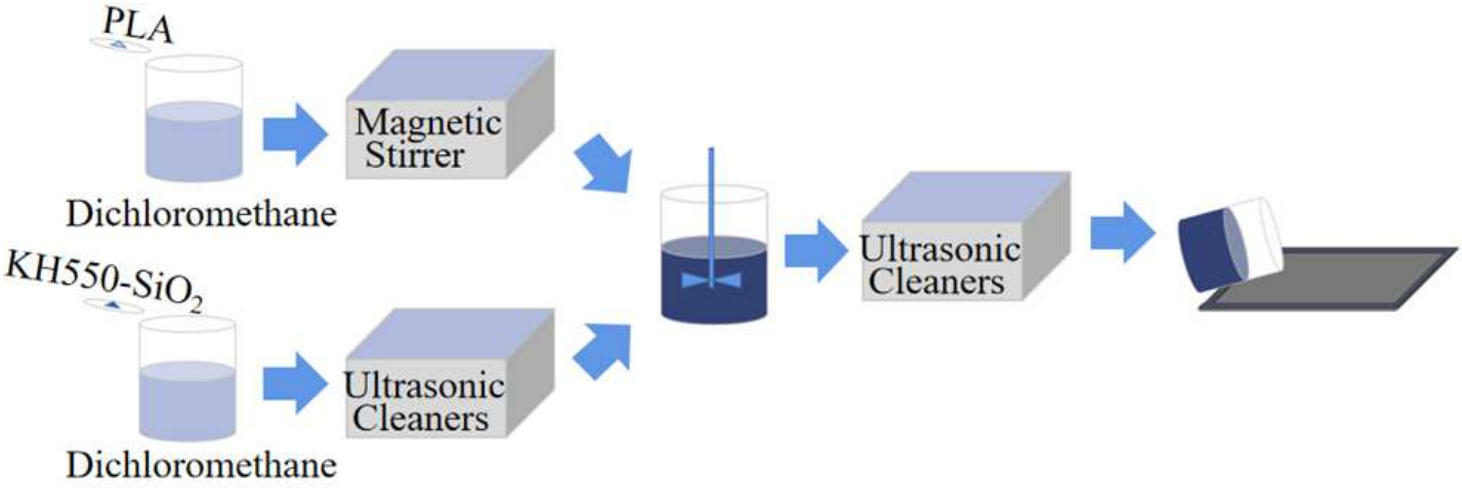

Figure 2

The scheme of preparation process of composite SiO2-PLA film

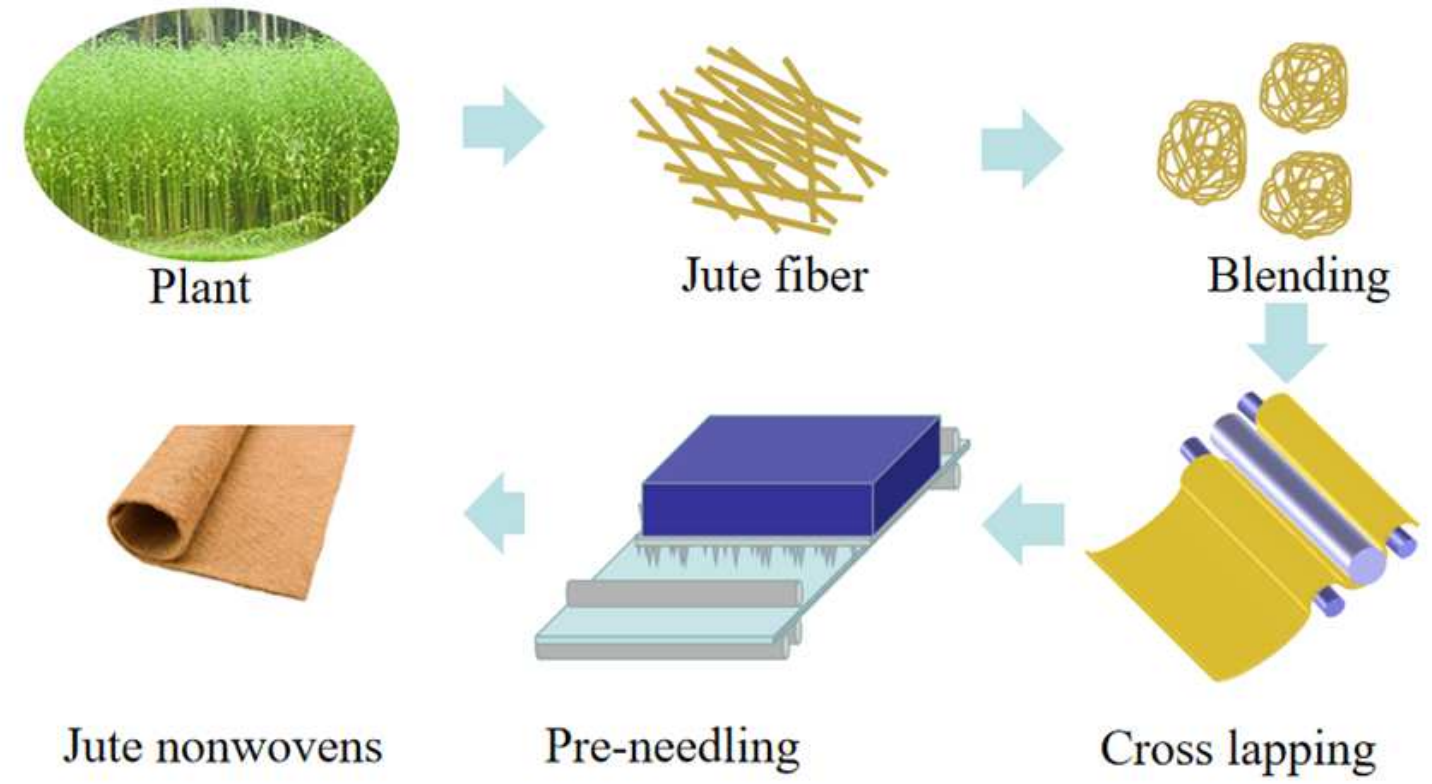

Figure 3

The preparation process of jute non-woven fabric

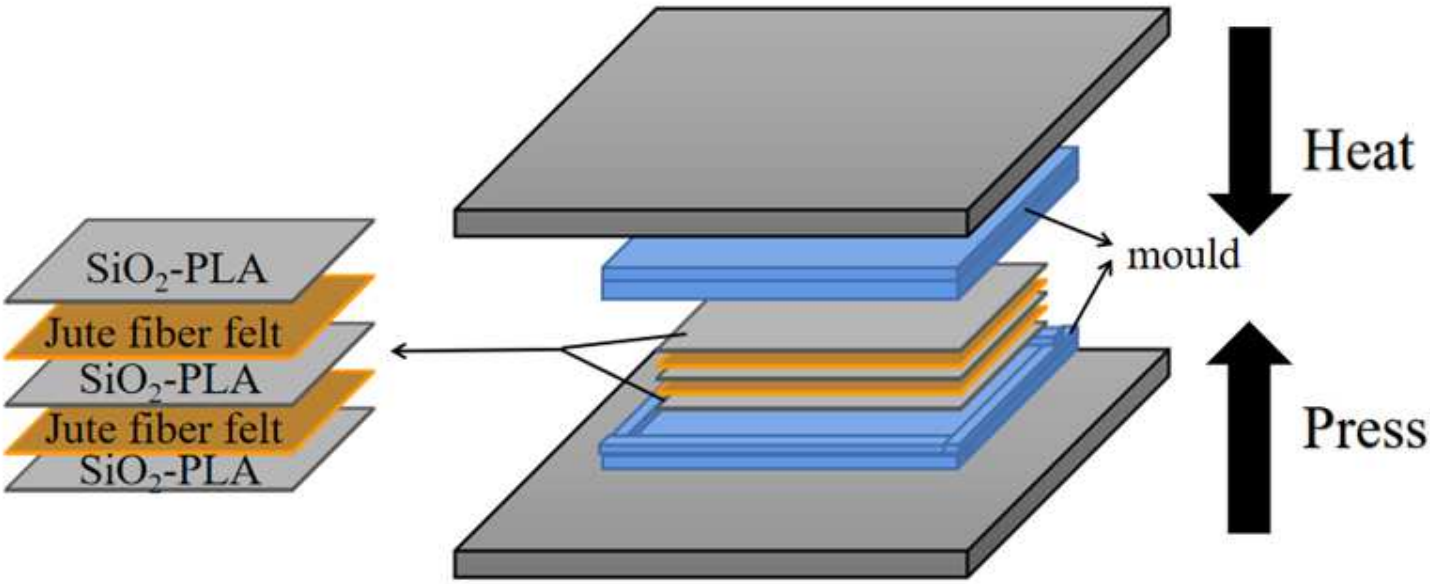

Figure 4

The preparation process of composite material

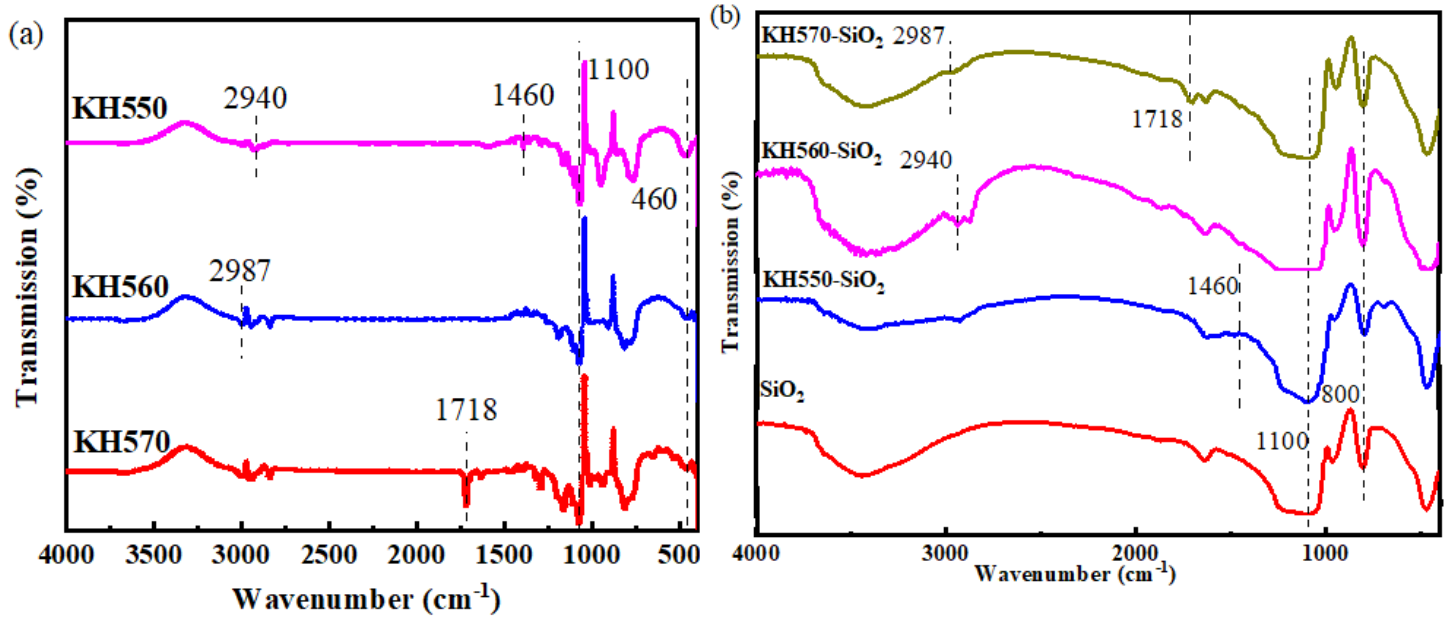

Figure 5

(a) FTIR spectra of KH550, KH560 and KH570; (b) FTIR spectra of SiO2, KH550-SiO2, KH560-SiO2 and KH570-SiO2 nanoparticle

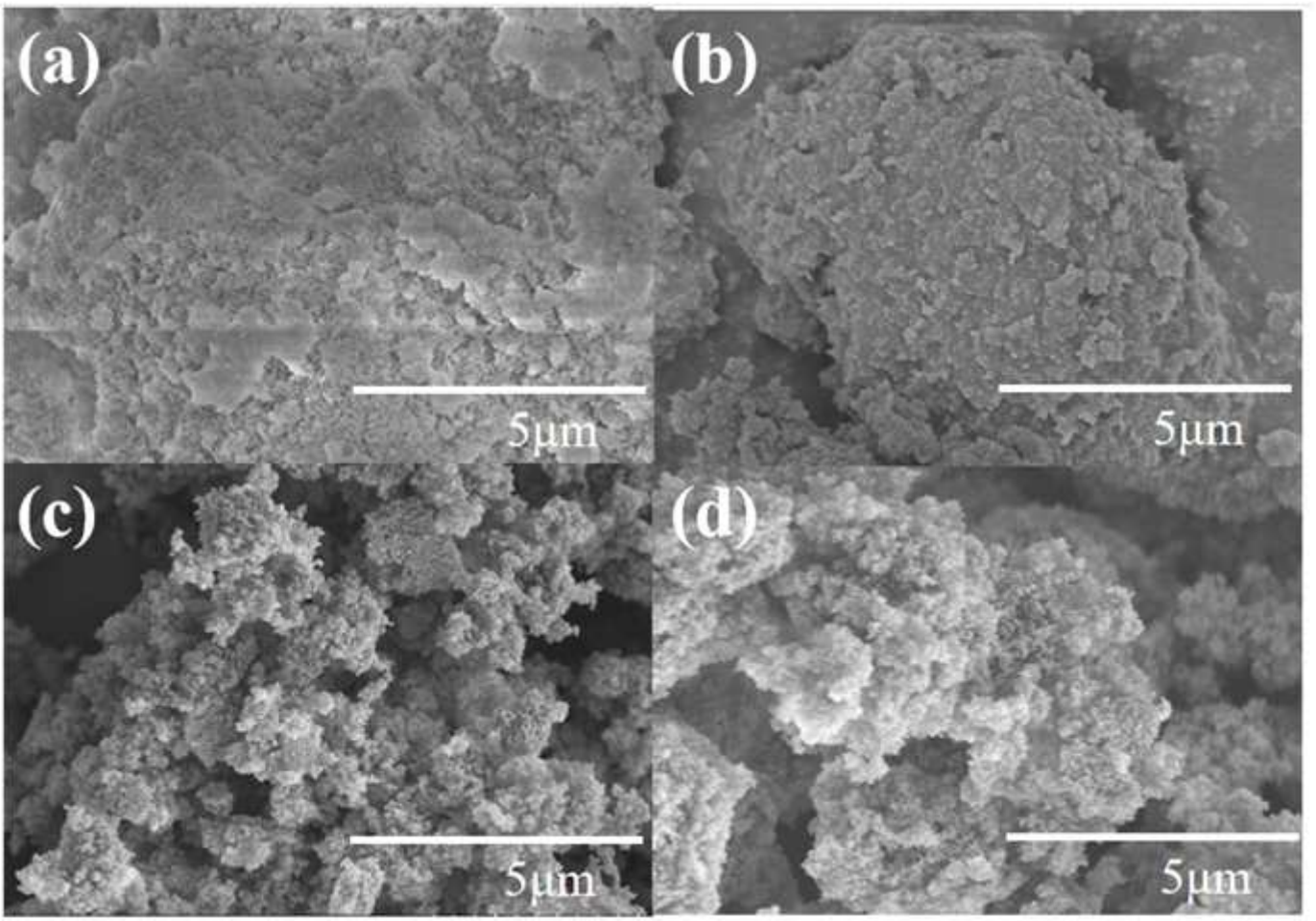

Figure 6

The surface morphology of SiO2. (a) SiO2; (b) SiO2-550; (c) SiO2-560; (d) SiO2-570

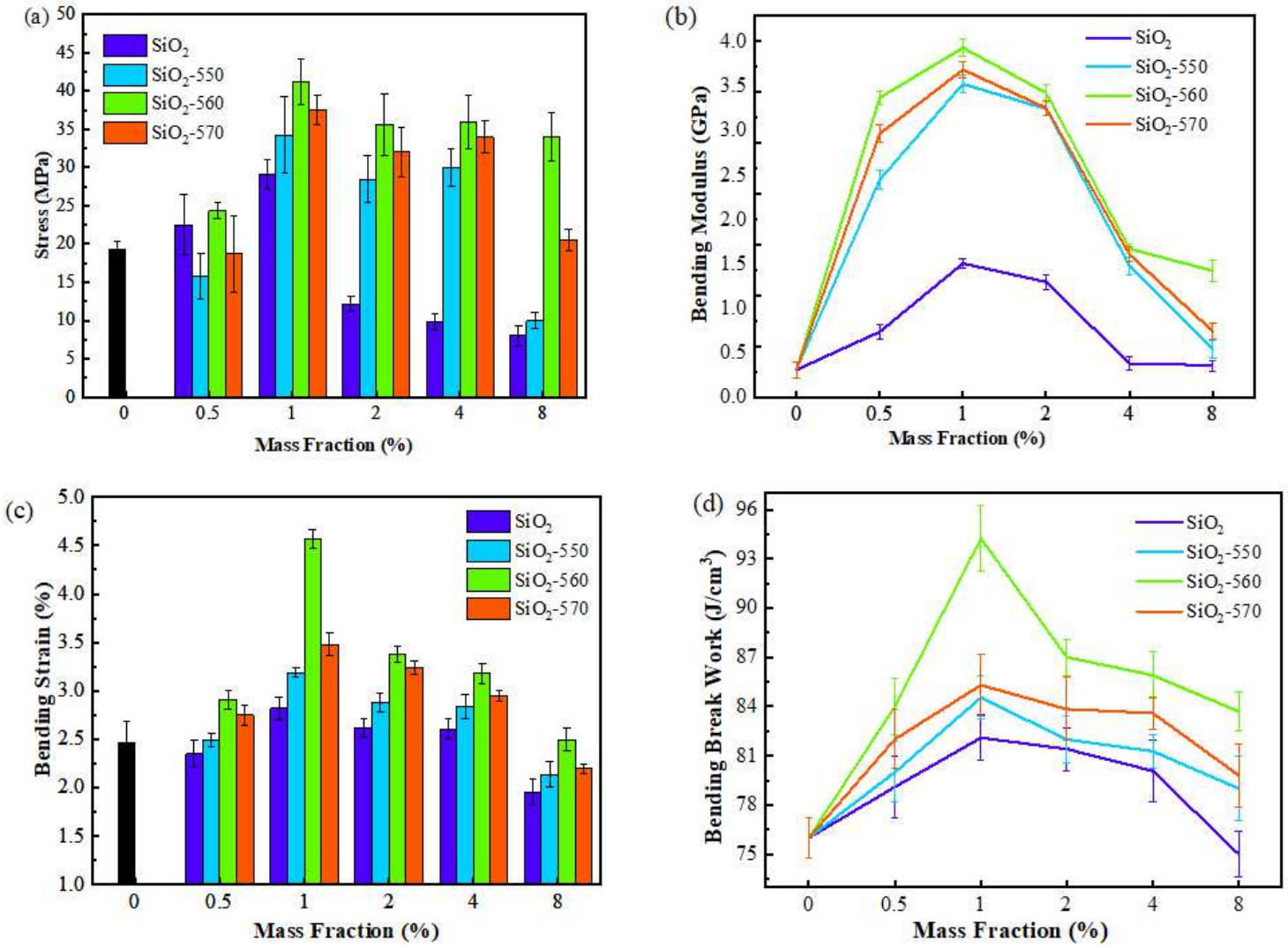

Figure 7

The effect of nano-SiO2 on tensile properties of jute/PLA composite bending performance. (a) Bending strength; (b) Modulus; (c) Bending strain; (d) Bending break work

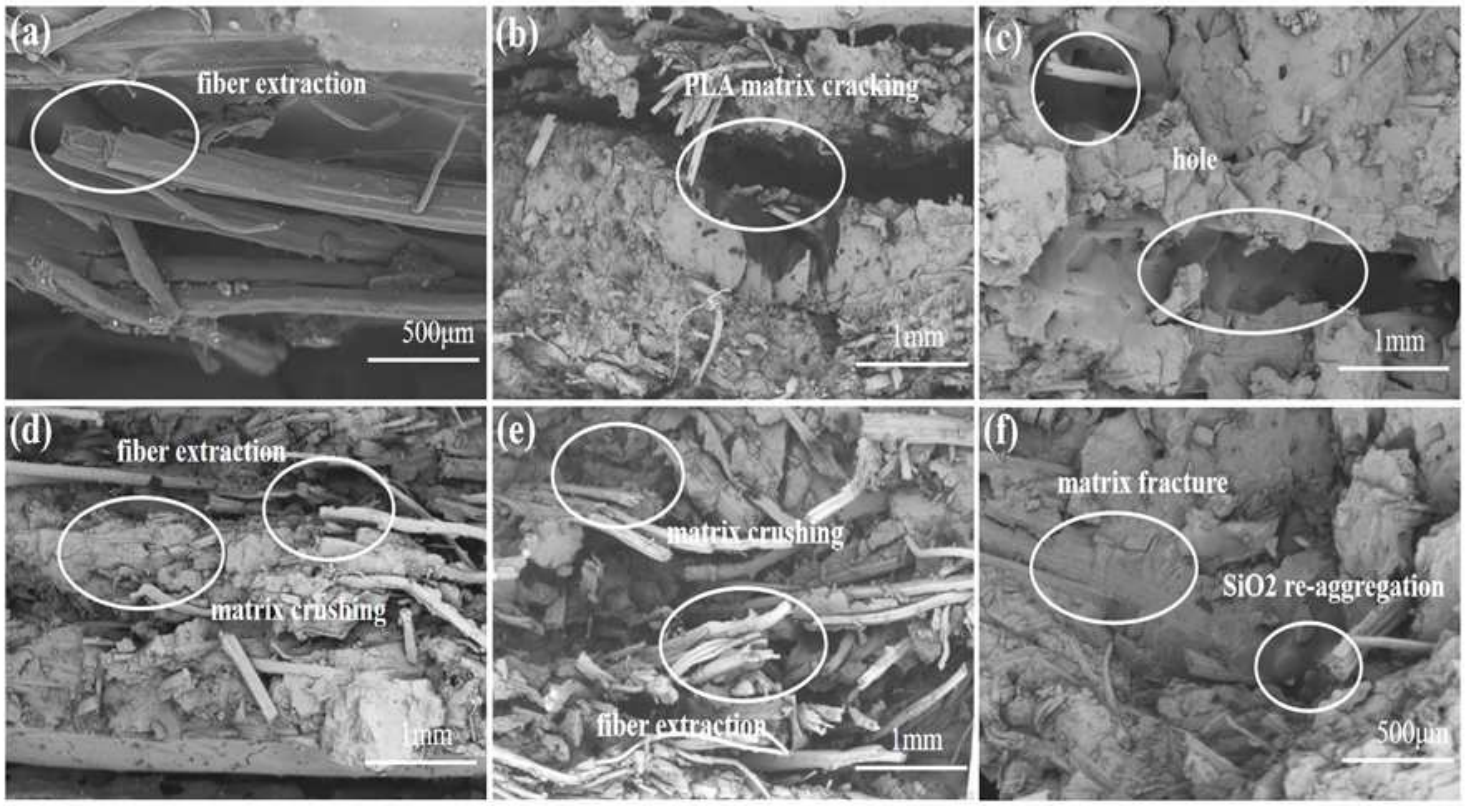

Figure 8

The fracture surface morphologies of jute/PLA composite (×200). (a) jute/PLA composite. (b) Sample 560-0.5. (c) Sample 560-1. (d) Sample 560-2. (e)Sample 560-4. (f) Sample 560-8

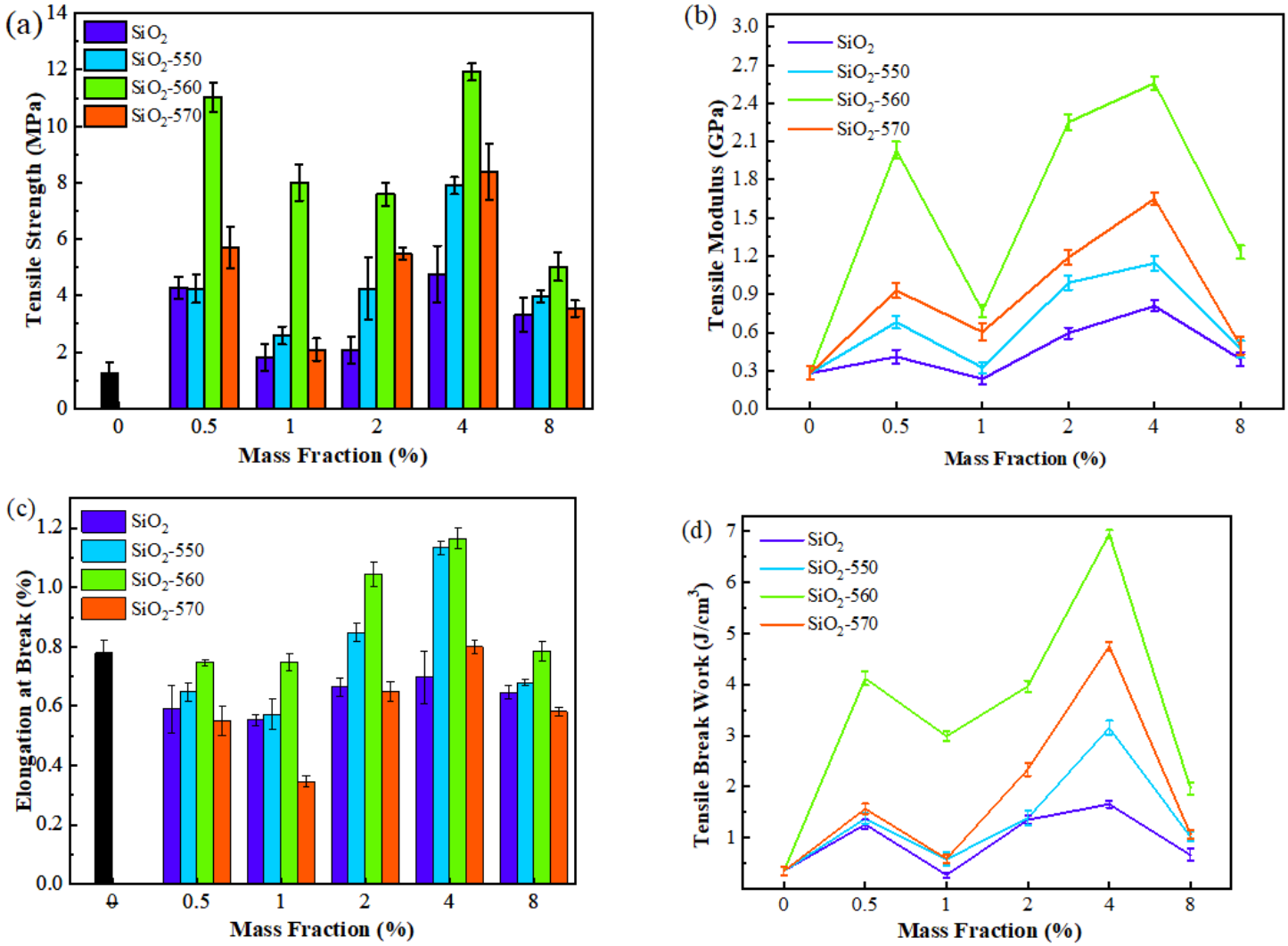

Figure 9

The effect of nano-SiO2 on tensile properties of jute/PLA fibers composites. (a) Tensile strength; (b)modulus; (c) Elongation at break; (d) Tensile break work

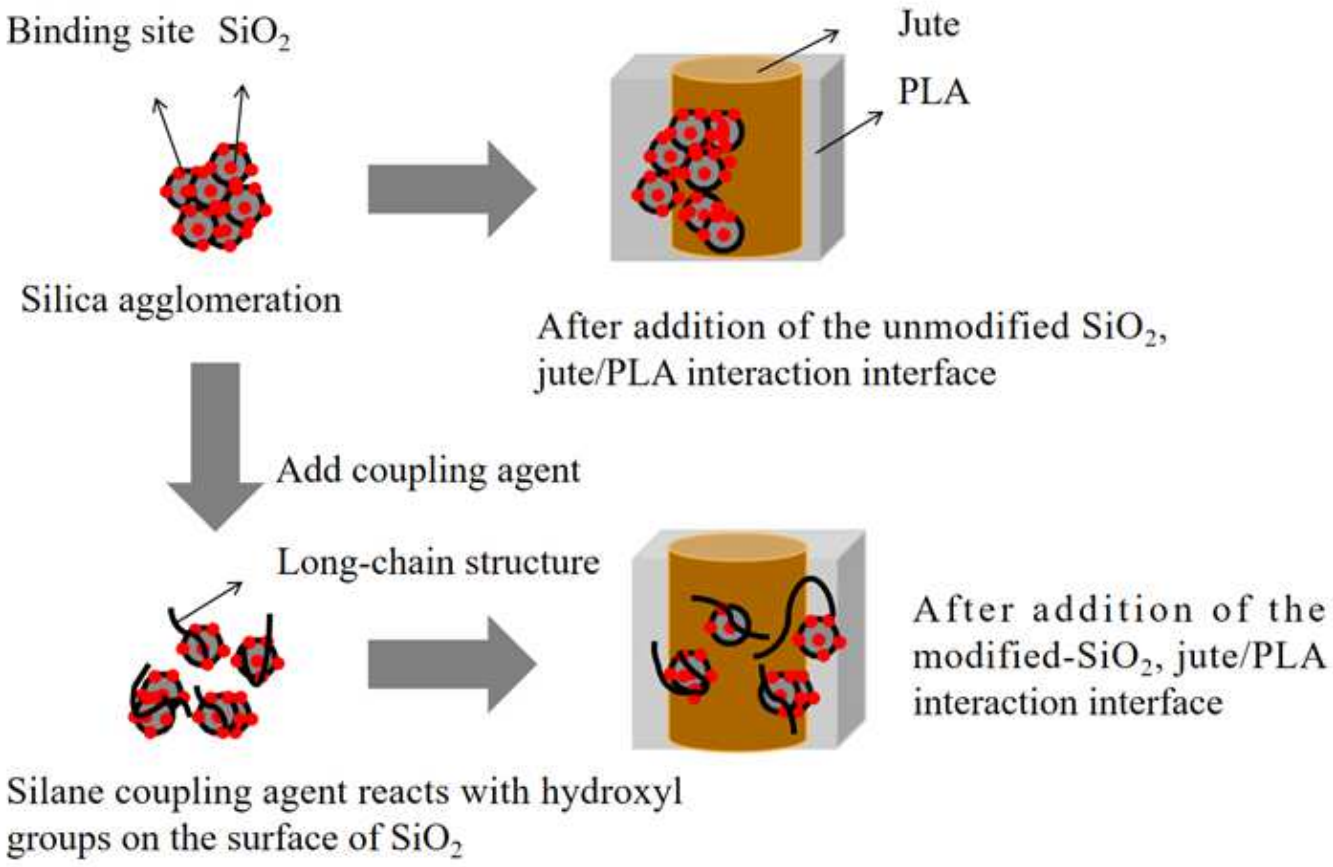

Figure 10

The interaction between the silica particles and the interface of the jute/PLA composite before and after the modification of the silane coupling agent.

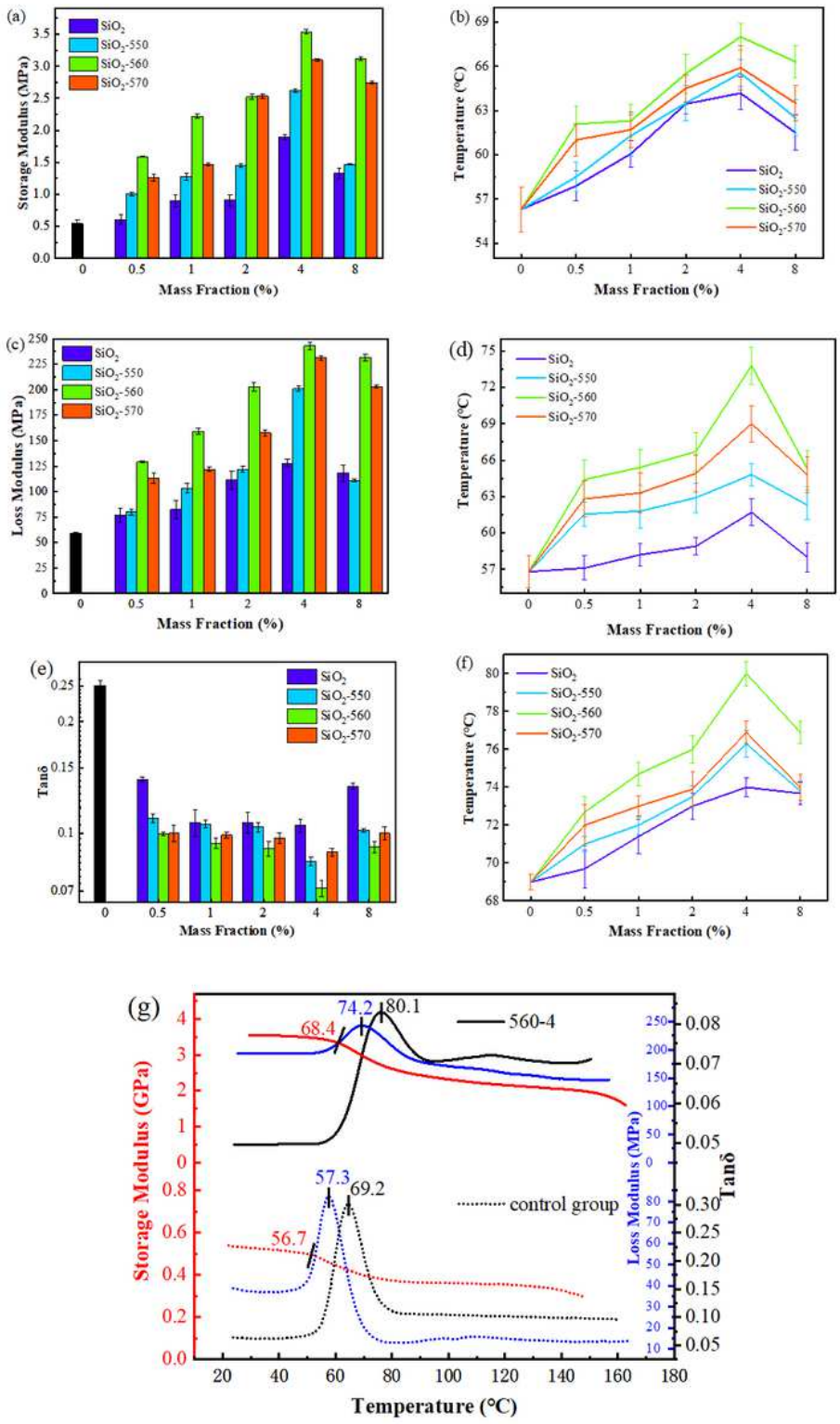

Figure 11

The DMTA of jute/PLA composite. (a) Storage modulus; (b) The temperature corresponding to storage modulus; (c) The maximum loss modulus; (d) The temperature corresponding to the maximum loss modulus; (e) The maximum tanδ; (f) The temperature corresponding to the maximum tanδ; (g) The comparison of DMTA between jute/PLA composite and sample 560-4

Supplementary Files

This is a list of supplementary files associated with this preprint. Click to download.

- renamed90625.doc